

Rotational Polymorphism in 2-Naphthalenethiol SAMs on Au(111)

Peng Jiang,^{†,‡} Aymeric Nion,[†] Alexandr Marchenko,[†] Luc Piot,[†] and Denis Fichou^{*,†}
CEA-Saclay, LRC Nanostructures et Semi-Conducteurs Organiques CNRS-CEA-UPMC, SPCSI/DRECAM,
91191 Gif-sur-Yvette, France, and National Center for Nanoscience and Technology (NCNST),
Beijing 100080, People's Republic of China

Received May 2, 2006; E-mail: denis.fichou@cea.fr

Self-assembled monolayers (SAMs) that spontaneously form on metal or semiconductor surfaces by organothiol derivatives currently attract great attention because of their ability to tailor interfaces and to be used in applications such as biosensors and electronic devices.¹ Among them, aromatic thiols are of considerable interest owing to the presence of an extended π -conjugated system.² For example, the charge-transfer process taking place between benzene-1,4-dithiol and metal electrodes has been investigated.³ Although the bidimensional morphology of SAMs is well-defined and can be investigated down to the molecular level, they often exhibit polymorphism, the coexistence of two or more crystallographic structures.⁴ Polymorphism can find applications in industrial applications such as pharmaceutical production and formulation. Like bulk polymorphs, 2D polymorphs may have different chemical and physical properties. Ishida et al. investigated the influence of the structural arrangement of biphenyl and terphenyl thiol compounds on their electrical conduction.⁵ Bratkovsky and Kornilovitch studied the effects of contact geometry and gating on current through SAMs of conjugated thiol molecules.⁶ Azzam et al. reported on the odd–even changes in the molecular arrangement and packing density of biphenyl-based thiol SAMs.⁷ These studies show that it is important to determine the precise conformation and orientation of individual molecules in monolayers of aromatic thiols.

2-Naphthalenethiol (2NT) is a simple aromatic molecule with an extended π -conjugated system whose electronic properties have been investigated as SAMs adsorbed on gold.⁸ 2-Anthracenethiol SAM on Au(111) has been studied by Käfer et al. using several spectroscopic techniques and scanning tunneling microscopy (STM).⁹ However, the local bidimensional structure of 2NT SAMs has never been studied by STM. Once it is immobilized on a gold substrate and assuming that the S–Au bond is nearly vertical,¹⁰ the naphthalene moiety can rotate around the S–C bond and adopt various orientations. As shown in Figure 1, three model geometries are possible: “standing” ($\phi = 0^\circ$), “facing” ($\phi = 90^\circ$), and “lying” ($\phi = 180^\circ$), with ϕ being the angle between the naphthalene plane and the gold surface. We report here on a refined STM study of 2NT SAMs at the *n*-tetradecane/Au(111) interface to determine the precise orientation of individual 2NT molecules on the Au substrate. STM at the liquid/solid interface allows imaging of SAMs in ambient conditions down to molecular resolution.¹¹ Two well-ordered 2NT phases having different close-packed arrangements are observed. Our study provides the first direct evidence of rotational polymorphism of 2NT molecules on Au(111).

Reconstructed Au(111) substrates are prepared by annealing Au thin films (~ 150 nm) vacuum deposited on a freshly cleaved mica foil (Goodfellow) in a propane–air flame. A microdroplet of a solution of 2NT (~ 0.05 mg/mL) in *n*-tetradecane (Aldrich, 99.99%) is deposited on a Au(111)/mica sample (5×5 mm²).¹¹ STM imaging is performed at the *n*-tetradecane/Au(111) interface using a

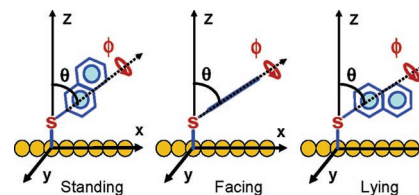


Figure 1. Three possible surface rotamers of 2NT molecules adsorbed on Au(111): standing (left, $\phi = 0^\circ$), facing (middle, $\phi = 90^\circ$), and lying (right, $\phi = 180^\circ$) as defined by the rotation angle ϕ of the naphthalene moiety around the axis of the S–C bond. Note that the tilt angle θ remains constant.

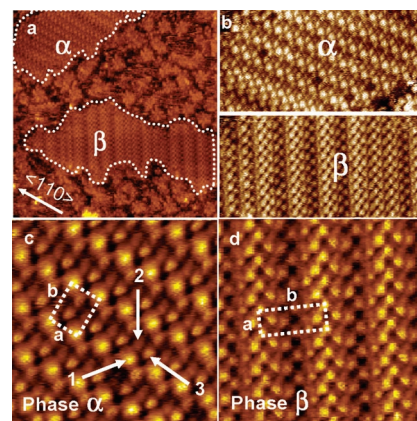


Figure 2. Typical STM images of the coexisting ordered phases (α and β) of 2NT monolayers on Au(111) at various scales. (a) 44×44 nm², $U_t = 0.5$ V, $I_t = 50$ pA; (b) (upper) phase α (16×8 nm², $U_t = 0.5$ V, $I_t = 18$ pA); (lower) phase β (18.3×9.1 nm², $U_t = 0.5$ V, $I_t = 50$ pA); (c) phase α (6.5×6.5 nm², $U_t = 0.5$ V, $I_t = 50$ pA); (d) phase β (8.5×8.5 nm², $U_t = 0.5$ V, $I_t = 100$ pA). Unit cells are shown as dashed white rectangles. In panel c, individual 2NT molecules indicated by arrows and numbered 1, 2, and 3 are adsorbed respectively on top, bridge, and 3-fold hollow positions of gold (see also Figure 3). In panel a, the $\langle 110 \rangle$ direction refers to the gold substrate.

Pico-SPM (Molecular Imaging/Agilent Technology) in constant-current mode at room temperature. Typical scanning parameters are 0.3–0.5 V for the tip voltage and 10–30 pA for tunneling current. After deposition of the 2NT solution on gold, the $(23 \times \sqrt{3})$ reconstructed herringbone structure of Au(111) is no longer visible (see Supporting Information (SI)).¹² Instead, the surface is covered by ordered domains with lateral sizes in the range 10–40 nm (Figure 2a). These domains are separated by randomly distributed depressions and smaller star-shaped domains with an average height ~ 0.24 nm and lateral sizes of 2–5 nm. The STM image in Figure 2a reveals that the large domains consist of highly ordered stripes (or lamellae) aligned along three preferential $\langle 110 \rangle$ directions rotated at 120° , reflecting the 3-fold symmetry of the underlying gold substrate. The $\langle 110 \rangle$ direction of Figure 2a is determined on a larger scale image of the same region showing a monatomic gold step edge. Two types of ordered phases, α and β , coexist in the SAMs (see Figure 2b). Both α and β phases are stable, occupy equal

[†] LRC Nanostructures et Semi-Conducteurs Organiques CNRS-CEA-UPMC.

[‡] National Center for Nanoscience and Technology.

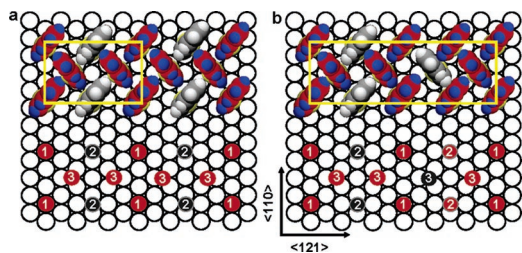


Figure 3. Top view of the proposed structural models for (a) the α -phase $3 \times 3\sqrt{3}R 30^\circ$ and (b) the β -phase $3 \times 6\sqrt{3}R 30^\circ$ of 2NT monolayers on Au(111). The herringbone arrangement is shown in the upper part and the position of sulfur atoms in the lower part. Molecules with standing orientations are in red, while those having the lying orientation are in black (see Figure 1). As in Figure 2c, 1, 2, and 3 label respectively the top, bridge, and 3-fold hollow sites of gold.

sample areas, and have constant sizes and shapes over time. The α -phase reveals three kinds of protrusions with different heights (labeled 1, 2, and 3 in Figure 2c). The geometry of these protrusions remains stable under imaging conditions ($|U| \cong 0.1\text{--}1\text{ V}$, $I_t = 0.01\text{--}0.1\text{ nA}$). On the basis of their lateral sizes, they are assumed to be individual 2NT molecules adsorbed on the Au(111) surface. Analysis of the cross-sectional profiles (see SI) along the $\langle 110 \rangle$ and $\langle 121 \rangle$ directions reveals an ordered $3 \times 3\sqrt{3}R 30^\circ$ structure with a rectangle unit cell ($a = 0.93 \pm 0.06\text{ nm}$; $b = 1.5 \pm 0.1\text{ nm}$; $\alpha = 90 \pm 2^\circ$). Through simple calculation, we find that the unit cell contains four molecules with an average area of $34.9\text{ \AA}^2/\text{molecule}$. Two of them stand in the center of the unit cell, the structure being thus $c(4 \times 2)$. In contrast to the 0.33 surface coverage of close-packed *n*-alkanethiol SAMs ($21.6\text{ \AA}^2/\text{molecule}$), the estimated value of 0.22 for 2NT on gold ($34.9\text{ \AA}^2/\text{molecule}$) implies a significantly less dense packing. Considering the van der Waals dimensions of a 2NT molecule ($7.6 \times 3.3\text{ \AA}^2$) and the average area per molecule, the apparent tilt angle can be estimated to be $\theta = \arcsin(25.1/34.9) \cong 44^\circ$ with respect to the surface normal, as schematized in Figure 1.

In the α -phase, the height difference between protrusions 1 and 2 is $\sim 1.0\text{ \AA}$, vs only $\sim 0.2\text{ \AA}$ between 1 and 3 (see SI). Considering the various possible orientations of the 2NT molecules and the different adsorption sites they can occupy on the gold lattice (top, bridge, and 3-fold hollow), a reasonable simplified packing model is proposed in Figure 3a. In this model, molecules arrange in a herringbone-type structure with the molecular mirror plane parallel to the $\langle 121 \rangle$ direction of the Au(111) surface.¹³ In the unit cell, 2NT molecules coexist in both standing and lying orientations because of the free rotation around the S–C bond. In both orientations, the naphthalene plane is nearly perpendicular to the substrate. Molecules in sites 1 and 3 (red in Figure 3) possess a standing orientation and occupy top and 3-fold hollow positions, respectively. Molecules in site 2 (in black in Figure 3) possess a lying orientation and occupy a bridge position. The unit cell of the α -domain contains three rotamers in standing orientation and one a lying. Finally, one cannot exclude a weak contribution of electronic effects to the apparent STM height of molecules in the various sites although this contribution is usually not dominant.⁷ Furthermore, the measured apparent heights are highly reproducible from sample to sample, with constant differences from one site to another.

In the β -phase, a $c(6 \times 2)$ superlattice has been identified and can be described by a $3 \times 6\sqrt{3}R 30^\circ$ rectangular unit cell ($a = 0.93 \pm 0.06\text{ nm}$, $b = 3.0 \pm 0.2\text{ nm}$, $\alpha = 90 \pm 2^\circ$) with eight molecules with the same average area ($34.9\text{ \AA}^2/\text{molecule}$) and surface coverage (0.22). The β -phase unit cell contains six molecules with a standing conformation and two lying. A 2D structural model for the superstructure is proposed in Figure 3b. Note that in the β -phase

unit cell molecules occupy similar sites as in phase α although three of them adopt different orientations (standing or lying).

Reports on aromatic thiols have shown that the SH headgroups can occupy various adsorption sites on Au(111).¹⁴ Theoretical investigations indicate that the energy difference between various geometries for thiol derivatives on Au(111) is extremely small.¹⁵ Thus, in addition to the usual chemical interaction between the Au and S atoms, it appears that the main factor controlling the formation of two phases and the coexistence of rotamers in 2NT SAMs is the geometry of the molecule. In addition, since in both the standing and lying rotamers the naphthalene plane is perpendicular to the gold surface, π – π interactions between 2NT molecules play a crucial role in the multifold, complex packing arrangement.

In conclusion, we have shown by STM that 2NT SAMs on Au(111) coexist as two stable phases (α and β) which possess molecules in two different orientations (standing and lying) according to the gold substrate. Such rotational polymorphism is observed and understood at the molecular level for the first time. High-resolution STM images reveal a $3 \times 3\sqrt{3}R 30^\circ$ structure for the α phase and a $3 \times 6\sqrt{3}R 30^\circ$ structure for the β phase whose unit cells contain, respectively, four and eight molecules. Both phases have the same average area per molecule (34.9 \AA^2) as well as surface coverage (0.22). Our findings open new perspectives in the precise control of 2D self-assembly of functionalized conjugated molecules. We are currently investigating the influence of rotational orientation of the 2NT molecules on their local transport properties by means of scanning tunneling spectroscopy.

Acknowledgment. This work has been performed at CEA-Saclay in the framework of an agreement between CEA-Saclay and the Chinese Academy of Sciences (CAS). P.J. thanks CEA-Saclay and the NCNST, China, for financial support.

Supporting Information Available: Additional STM images. This material is available free of charge via the Internet at <http://pubs.acs.org>.

References

- (1) (a) Dubois, L. H.; Nuzzo, R. G. *Annu. Rev. Phys. Chem.* **1992**, *43*, 437–463. (b) Jiang, P.; Liu, Z.-F.; Cai, S.-M. *Appl. Phys. Lett.* **1999**, *75*, 3023–3025. (c) Schreiber, F. *Prog. Surf. Sci.* **2000**, *65*, 151–256. (d) Love J. C.; Estroff L. A.; Kriebel J. K.; Nuzzo R. G.; Whitesides G. M. *Chem. Rev.* **2005**, *105*, 1103–1169.
- (2) (a) Chadwick, J. E.; Myles D. C.; Garrell, R. L. *J. Am. Chem. Soc.* **1993**, *115*, 10364–10365. (b) Dhirani, Al-A.; Zehner, R. W.; Hsung, R. P.; Guyot-Sionnest, P.; Sita, L. R. *J. Am. Chem. Soc.* **1996**, *118*, 3319–3320. (c) Yang, G.; Liu, G. Y. *J. Phys. Chem. B* **2003**, *107*, 8746–8759.
- (3) Chen, J.; Reed, M. A.; Rawlett, M. A.; Tour, J. M. *Science* **1999**, *286*, 1550–1552.
- (4) Bernstein, J.; Davey, R. J.; Henck, J. O. *Angew. Chem., Int. Ed.* **1999**, *38*, 3441–3461.
- (5) Ishida, T.; Mizutani, W.; Choi, N.; Akiba, U.; Fujihira, M.; Tokumoto, H. *J. Phys. Chem. B* **2000**, *104*, 11680–11688.
- (6) Bratkovsky, A. M.; Kornilovitch, P. E. *Phys. Rev. B* **2003**, *67*, 115307.
- (7) (a) Azzam, W.; Cyganik, P.; Witte, G.; Buck, M.; Wöll, C. *Langmuir* **2003**, *19*, 8262–8270. (b) Azzam, W.; Fuxen, C.; Birkner, A.; Rong, H.-T.; Buck, M.; Wöll, C. *Langmuir* **2003**, *19*, 4958–4968.
- (8) (a) Kolega, R. R.; Schlenoff, B. J. *Langmuir* **1998**, *14*, 5469–5478. (b) Ganesh, V.; Lakshminarayanan, V. *J. Phys. Chem. B* **2005**, *109*, 16372–16381. (c) Ouyang, J. Y.; Chu, C. W.; Sieves, D.; Yang, Y. *Appl. Phys. Lett.* **2005**, *86*, 123507.
- (9) Käfer, D.; Witte, G.; Cyganik, P.; Terfort, A.; Wöll, C. *J. Am. Chem. Soc.* **2006**, *128*, 1723–1732.
- (10) Ulman, A. *Chem. Rev.* **1996**, *96*, 1533–1554.
- (11) (a) Marchenko, A.; Katsonis, N.; Fichou, D.; Aubert, C.; Malacria, M. *J. Am. Chem. Soc.* **2002**, *124*, 9998–9999. (b) Katsonis, N.; Marchenko, A.; Fichou, D. *J. Am. Chem. Soc.* **2003**, *125*, 13682–13683. (c) Piot L.; Marchenko, A.; Wu J. S.; Müllen K.; Fichou, D. *J. Am. Chem. Soc.* **2005**, *127*, 16245–16250.
- (12) Barth, J. V.; Brune, H.; Ertl, G.; Behm, R. J. *Phys. Rev. B* **1990**, *42*, 9307–9318.
- (13) Chang, C. C.; Chao, I.; Tao, Y. T. *J. Am. Chem. Soc.* **1994**, *116*, 6792.
- (14) (a) Yang, G.; Qian, Y.; Engtrakul, C.; Sita, L. R.; Liu, G. Y. *J. Phys. Chem. B* **2000**, *104*, 9059–9062. (b) Kang, J. F.; Ulman, A.; Liao, S.; Jordan, R.; Yang, G.; Liu, G. Y. *Langmuir* **2001**, *17*, 95–106.
- (15) Gottschalck, J.; Hammer, B. *J. Chem. Phys.* **2002**, *116*, 784–790.

JA063060Z